

Extreme elongation of asteroid 1620 Geographos from radar images

S. J. Ostro*, K. D. Rosema*, R. S. Hudson†, R. F. Jurgens*, J. D. Giorgini*, R. Winkler*,
D. K. Yeomans*, D. Choate*, R. Rose*, M. A. Slade*, S. D. Howard*, & D. L. Mitchell*

* Jet Propulsion Laboratory, California Institute of Technology, Pasadena, California 91109-8099, USA

† School of Electrical Engineering and Computer Science, Washington State University, Pullman,
Washington 99164-2752, USA

To be submitted to *Nature*

March 1995

The shapes of Earth-crossing asteroids provide insight into their origin. However, these objects are generally unresolved with optical telescopes and shape constraints from disc-integrated lightcurves are subject to large systematic sources of bias¹. Here we present initial results of delay-Doppler radar observations of 1620 Geographos which reveal this object's pole-on silhouette at ~100-m resolution. The silhouette is irregular, nonconvex, and apparently monolithic with overall dimensions, 5.11 ± 0.15 km and 1.85 ± 0.15 km, whose ratio, 2.76 ± 0.21 , establishes Geographos as the most elongated solar system object imaged so far. Small asteroids are thought to be the outcome of catastrophic collisions², but laboratory experiments^{3,4} yield fragment elongations that average about 1.4, with fewer than 1% as elongated as Geographos. The origin of this object's shape probably involves phenomena or circumstances that have yet to be simulated accurately and may be unique among the known asteroids.

In August 1994, asteroid 1620 Geographos passed within 0.03 AU of Earth, its closest approach for at least the next two centuries. The asteroid entered the declination window of the Goldstone radar on Aug. 28 and we observed it daily for one week, obtaining hundreds of delay-Doppler images. Here we present the first results from our highest-resolution observations.

A delay-Doppler image cuts a target into cells that are parallel to the apparent spin vector's plane-of-sky projection⁵. Constraints^{6,7} on Geographos' pole direction from optical lightcurves indicate that Goldstone was within 10° of the asteroid's equatorial plane throughout the radar observations, so the delay-Doppler cells remain nearly normal to the asteroid's equatorial plane at all rotation phases. Since each cell can capture echoes from surface regions north and south of the equator, an image is a "double exposure" that contains an intrinsic north/south ambiguity. However, sums of images over a sufficient range of phases can unambiguously define the asteroid's pole-on silhouette, i.e., the outline of the object when viewed from along the pole.

Our highest-resolution observations consisted of 250 runs on Aug. 30-31 (Table 1). In each run, Goldstone's 70-m antenna (DSS 14) transmitted a 450-kW signal for about 50s and then received echoes for a somewhat shorter duration. The transmission was a repetitive, binary-phase-coded continuous-wave signal⁸ with a 127-element code and a 0.5-μs time resolution that provided 75-m range resolution. Real-time processing of received signals, which included digitization, decoding, and spectral analysis, yielded arrays of echo power in 127 delay bins and 64, 1.64-Hz frequency bins. The length equivalent (87 m) of the frequency resolution and our rotation-phase assignments were calculated from a topocentric ephemeris and comprehensive, lightcurve-based estimates (P. Magnusson, pers.comm.) of the spin period ($5.22332784 \pm 0.00000096$ h) and pole direction (ecliptic longitude, latitude = $55^\circ \pm 5^\circ, -45^\circ \pm 50^\circ$); relative errors in our phase assignments are thought to be very small compared to the 0.6° phase resolution of

each run. Our phase origin corresponds to the asteroid's end-on orientation near primary (dimpest) lightcurve minimum $m1$, which follows primary (brightest) lightcurve maximum $M1$. Geographos lightcurves show extrema in the chronological order $m1, M2, m2, M1$, corresponding to phases $\theta = 0^\circ, 90^\circ, 180^\circ$, and 270° .

The extremely high noise level in images from individual runs is reduced by an order of magnitude when all the runs from a given date are summed. Our precise knowledge of the spin period makes rotational co-registration of images straightforward. Of more concern is "translational smearing" caused by imperfect knowledge of the delay-Doppler location of the center of mass (COM) from image to image. Our prediction ephemerides were accurate enough to prevent perceptible smearing over time scales of order 10 min, but much longer summations require an *a posteriori* ephemeris that is at least two orders of magnitude more accurate.

Preliminary application of several analysis methods^{10,11} to low-resolution data from Aug. 28 - Sep. 2 has produced an ephemeris for which the COM trajectory during Aug. 30-31 is believed to contain uncertainties that degrade the data's intrinsic resolution by no more than several tens of percent on each day.

Figure 1 shows estimates of Geographos' pole-on silhouette from co-registration and summation of single-run images. The echoes were stronger and the phase coverage was better on Aug. 30, but the two estimates are in excellent agreement. Our estimates of the silhouette's extreme breadths are: 5.11 ± 0.15 km and 1.85 ± 0.15 km; the stated uncertainties are subjective standard errors. Our estimate of the asteroid's elongation (i.e., the ratio of the silhouette's extreme breadths) is: $\beta = 2.76 \pm 0.21$; we have assumed a cross correlation coefficient¹² of 0.5 between uncertainties in the breadth estimates, because they suffer similar biases from errors in the *a posteriori* ephemeris. These results show that lightcurve-based predictions^{6,7} about Geographos' elongation were accurate. They also support the general conclusion resulting from

the Galileo spacecraft flybys of the much larger, main-belt asteroids 951 Gaspra¹³ and 243 Ida¹⁴ that shape models based upon well determined lightcurves^{15,16} are reliable predictors of those objects' elongations.

How rare is Geographos' elongation among the Earth-crossing asteroids (ECAs) and main-belt asteroids of similar size? Lightcurve amplitudes (Δm magnitudes) are available for dozens of ECAS and small main-belt asteroids (MBAs), and $10^{0.4\Delta m}$ is often taken as a crude estimator of elongation despite the potentially strong dependence of Δm on viewing/illumination geometry¹. Binzel *et al.*¹⁷ studied a subset of those objects and noted that whereas amplitudes taken at face value implied mean elongations of ~ 1.6 for 32 ECAS and ~ 1.3 for 32 small MBAs, mean elongations between 1.2 and 1.3 were inferred for both groups if "global" corrections were applied to the amplitudes to compensate for primary sources of bias. Radar delay-Doppler and Doppler-only images (e.g., Ostro *et al.*^{18,19} and Ref. 11) have yielded direct determinations of β for about a dozen ECAs. Those asteroids, as well as 243 Ida^{14,21}, and all other solar system objects for which β has been measured from optical images^{22,23} are less elongated than Geographos.

What can be said about the detailed sequence of collisional events that produced Geographos' remarkable elongation? Apart from the silhouette's gross dimensions, one of its most interesting attributes is the disparity between the contours of its two long sides. The middle of the *M1* side contains a prominent indentation, but the entire length of the *M2* side is nearly convex at the 100-m scale. The silhouette's shape seems more suggestive of a monolithic fragment derived from a disruptive collision than a compound, multi-component product of a constructive collision.

Current understanding of collisional processes rests largely on hypervelocity

fragmentation experiments and theoretical scaling laws³⁴. Laboratory experiments have involved a wide range of impact velocities and target/projectile materials^{24,26}, and extrapolation to asteroidal scales is thought to have a modicum of validity^{27,28}. However, mean fragment elongations from those experiments are typically ~ 1.4 , with fewer than 1% as elongated as Geographos. Fragments from open-air detonation of spherical targets by contact charges²⁹ had mean elongations ~ 1.7 and several percent of them were more elongated than Geographos, suggesting that breakage of fragments against chamber walls in experiments not carried out in the open might bias results toward smaller elongations. On the other hand, small asteroids are thought to be the product of several generations of disruptive collisions so that experiments involving secondary fragmentation against chamber walls may provide the more relevant results. Capaccioni *et al.*²⁸ noted a tendency for fragments generated farther from the impact point to become larger and possibly more irregular in shape, and Paolicchi *et al.*³⁰ suggested that elongated fragments may be more likely if the collision-induced velocity field is highly asymmetric, but other clues to how elongated fragments might form are lacking. With an elongation value well above the mean, Geographos' figure may be the outcome of a rare combination of physical phenomena or circumstances that have yet to be simulated accurately.

References

1. Zappalà, V., Cellino, A., Barucci, M. A., Fulchignoni, M., & Lupishko, D. F. *Astron. Astrophys.* **231**, 548-560 (1990).
2. Farinella, P., Paolichi, P., & Zappalà, V. *Icarus* 52,409-433 (1982).
3. Fujiwara, A. *et al.* in *Asteroids* (eds Binzel, R. P., Gehrels, T., & Matthews, M. S.) 240-265 (Univ. of Arizona Press, Tucson, 1989).
4. Nakamura, A. *Laboratory studies on the velocity of fragments from impact disruption* (ISAS Rpt. 651, Institute of Space and Astronautical Science, Yoshinodai Sagamihara, Kanagawa, Japan, 1993).
5. Hudson, R. S. *Remote Sensing Reviews* **8**, 195-203 (1993).
6. Dunlap, J. L. *Astron. J.* 79,324-332 (1974).
7. Kwiatkowski, T. *Astron. Astroph.* 294,274-277 (1995).
8. Ostro, S. J. *Reviews of Modern Physics* **65**, 1235-1279 (1993).
9. Priest, P. *Goldstone Solar System Radar Capability and Performance* (JPL Internal Rpt. 1740-4, Jet Propulsion Laboratory, Pasadena 91109-8099, 1993).
10. Ostro, S. J., Connelly, R., & Belkora, L. *Icarus* 73, 15-24 (1988).
11. Hudson, R. S., & Ostro, S. J. *Science* **263**,940-943 (1994).
12. Finney, D. J. *Statistical Method in Biological Assay* 2nd edn (Hafner, New York, 1964).
13. Belton, M. J. S. *et al. Science* **257**, 1647-1652 (1992).
14. Belton, M. J. S., *et al. Science* 265, 1543-1547 (1994).
15. Magnusson, P. M. *et al. Icarus* 97, 124-129 (1992).
16. Binzel, R. P. *et al. Icarus* 105,310-325 (1993).
17. Binzel, R. P., Xu, S., Bus, S. J., & Bowell, E. *Science* 257,779-782 (1992).
18. Ostro, S. J. *et al. Astron. J.* 99,2012-2018 (1990).

19. Ostro, S. J. *et al. Astron. J.* 88,565-576 (1983).
20. Thomas, P.C. *et al. Icarus* 107, 23-36(1993).
21. Thomas, P. *et al. (abstr.) Bull. Am. Astron. Soc.* 26, 1155 (1994).
22. Burns, J. A. in *Satellites* (ed Burns, J. A.) 1-38 (Univ. of Arizona Press, Tucson, 1986).
23. Rahe, J., Vanysek, V., & Weissman, P. R. in *Hazards Due to Comets and Asteroids* (ed Gehrels, T.) 597-634 (Univ. of Arizona Press, Tucson, 1994).
24. Gault, D. E., & Wedekind, J. A. *J. Geophys. Res.* 74,6780-6794 (1969).
25. Cerroni, P. *Mem. S. A. It.* 57, 13-45 (1986).
26. Fujiwara, A. *Mm. S. A. It.* 57,47-64 (1986).
27. Fujiwara, A., Kamimoto, G., & Tsukamoto, A. *Nature* 272, 602-603 (1978).
28. Capaccioni, F. *et al. Icarus* 66, 487-514(1986).
29. GIBLIN, I. *et al. Icarus* **110,203-224 (1994).**
- 30. Paolichi, P., Cellino, A., Farinella, P., & Zappalà, V. *Icarus* 77, 187-212 (1989).**

ACKNOWLEDGEMENTS. We thank the Goldstone technical staff for their support of these observations. Part of this research was conducted at the Jet Propulsion Laboratory, California Institute of Technology, under contract with the National Aeronautics and Space Administration (NASA).

TABLE 1 Observation parameters

Aug . Date	Runs	UTC Interval (hh:mm - hh:mm)	Phase Interval
30	3	05:15 - 05:20	310° - 315°
"	43	05:23 - 07:07	320° - 64°
"	50	07:13 - 09:02	86° - 211°
"	21	09:07 - 10:01	218° - 279°
31	21	03:39 - 04:30	59° - 120°
"	52	05:43 - 07:28	202° - 322°
"	54	07:38 - 09:27	335° - 99°
...	-----	-----	-----

Columns give the number of runs, the UTC time interval, and the rotation-phase interval for each sequence of 0.5- μ s imaging runs during Aug. 30-31. Breaks between sequences were either caused by equipment problems or introduced to allow data transfer between acquisition and analysis computers. Geographos' **topocentric** right ascension, declination, and distance near the middle of the observations on Aug. (30, 31) were (321.6°, 321.70), (-23°, -180), and (0.048, 0.053 AU). All observations employed transmission of a circularly polarized signal and reception of echoes in the orthogonal circular (OC) polarization.

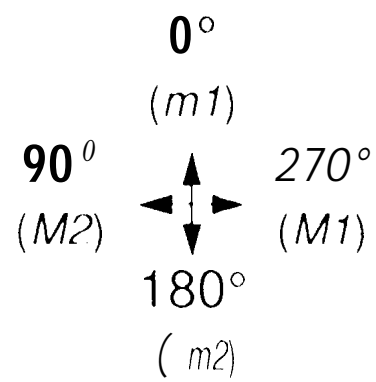
Caption

FIG. 1 Estimates of Geographos' pole-on silhouette from co-registration and summation of all 0.5- μ s images obtained on Aug. 30 and 31. The salient information in this image is the periphery of the echo distribution; the grayscale is arbitrary and no meaning is attached to brightness variations inside the silhouette. The tic marks on the borders are 1 km apart. The central white pixel in the single-date images locates the asteroid's center of mass. Labels indicate the radar's direction at rotation phases corresponding to lightcurve extrema.



Aug. 30

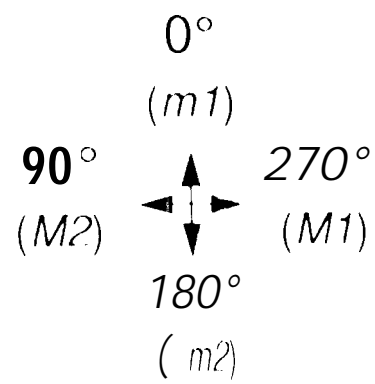
Aug. 31





Aug. 30

Aug. 31



Ostio et al. Fig. 1